$b\,^1\Sigma_g^+ - X\,^3\Sigma_g^-$ (0,0) band of oxygen isotopomers in relation to tests of the symmetrization postulate in $^{16}O_2$

H. Naus, A. de Lange, and W. Ubachs
Laser Centre, Department of Physics and Astronomy, Vrije Universiteit, De Boelelaan 1081, 1081 HV Amsterdam, The Netherlands
(Received 8 August 1997)

We investigated the $b\,^1\Sigma_g^+ - X\,^3\Sigma_g^-$ (0,0) band of the $^{16}O^{18}O$, $^{16}O^{17}O$, $^{18}O_2$, $^{17}O^{18}O$, and $^{17}O_2$ isotopomers of oxygen. The weak magnetic dipole transitions around 760 nm were observed using cavity-ring-down absorption spectroscopy. The positions of over 340 lines are presented together with (re-) analyses of the rotational constants. We discuss the importance of these data in view of tests of the symmetrization postulate in $^{16}O_2$ and present a sensitivity scale of 13 orders of magnitude that could be practical for future test experiments. [S1050-2947(97)07812-8]

PACS number(s): 33.20.−t, 31.30.Gs, 05.30.Jp, 42.62.Fi

I. INTRODUCTION

The so-called oxygen ''*A* band,'' corresponding to the $b\,^1\Sigma_g^+ - X\,^3\Sigma_g^-$ (0,0) band at 760 nm, is the most prominent near-infrared absorption feature in the Earth's atmosphere. This *A* band is highly forbidden, since it is a gerade-gerade, Σ^+-Σ^-, and a singlet-triplet transition. With an Einstein *A* coefficient of 0.0887 s^{-1} [1] the four allowed branches in the magnetic dipole transition are a factor of 10^9 weaker than typical electric-dipole-allowed transitions.

Recently this oxygen *A* band has been used for a test of the symmetrization postulate of quantum mechanics in the $^{16}O_2$ molecule [2,3]. Since the early observations of the spectra of molecular oxygen it has been recognized that transitions starting from even rotational quantum states of $^{16}O_2$ were missing [4]. This phenomenon was explained by Heisenberg [5] to be a consequence of the symmetrization postulate for identical spin-0 nuclei. The ^{16}O nuclei in this homonuclear molecule are spin-0 particles, and quantum statistics rules that its molecular wave function must be totally symmetric under permutation of the nuclei. As a consequence, states with an even rotational angular momentum cannot exist, or cannot be populated. For a detailed explanation we refer to Herzberg [6] and Bunker [7]. This well-known phenomenon may be used as a test of the symmetrization postulate, in search of weak signals on transitions originating from such symmetry-forbidden states. In two recent experiments upper limits for a violation of the postulate have been set to 5×10^{-7} [2] and 8×10^{-7} [3], using techniques of frequency-modulated absorption and tunable diode lasers. In one of these studies [2] transitions in $^{16}O^{18}O$ and $^{16}O^{17}O$ were explicitly studied. Magnetic dipole transitions in $^{18}O_2$ or electric quadrupole transitions in $^{16}O_2$ [8], which should be observable at the 5×10^{-7} sensitivity level were not included in these studies.

In the present work we report on observations on the oxygen *A* band, using cavity-ring-down spectroscopy. This technique has in recent years been developed into a versatile and sensitive spectroscopic tool for measuring weak absorptions or low concentrations [9–14]. The *A* band of the isotopomers $^{16}O^{18}O$, $^{16}O^{17}O$, $^{18}O_2$, $^{17}O^{18}O$, and $^{17}O_2$ was studied in isotopically enriched samples, resulting in line positions with an accuracy of 0.03 cm^{-1}. Knowledge of the spectral positions of all isotopomer lines will ascertain that no coincidences occur between weak signals from isotopomer lines and the position of lines in $^{16}O_2$ selected for search procedures to test the symmetrization postulate. Furthermore, an electric quadrupole line in $^{16}O_2$ was observed, which is known to have a line strength of 3×10^{-6} with respect to the magnetic dipole transitions [8], setting our present sensitivity limit at 1.5×10^{-6}. Based on the known natural abundances of the rare oxygen isotopomers in conjunction with the electric quadrupole transitions a sensitivity scale is established that may be of use in future work testing a possible violation of the symmetrization postulate in $^{16}O_2$.

II. EXPERIMENT

Our experimental setup is displayed schematically in Fig. 1. Wavelength tunable pulsed laser radiation (5 ns) near 760 nm is used in a typical cavity-ring-down spectroscopy

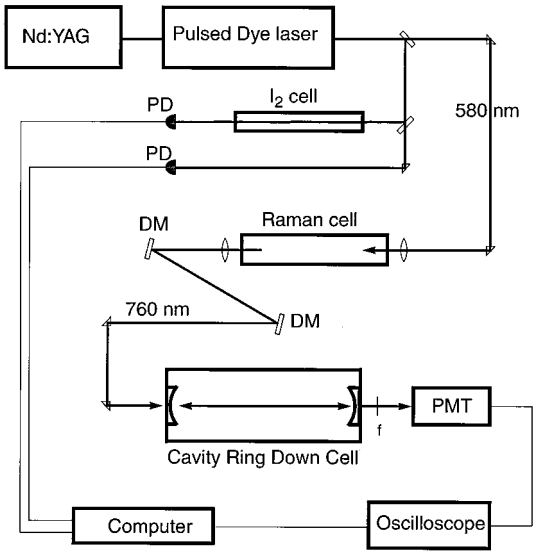

FIG. 1. Schematic display of the experimental setup: PD, photodiodes; DM, dichroic mirrors for separation of the Raman-shifted wavelength from the fundamental.

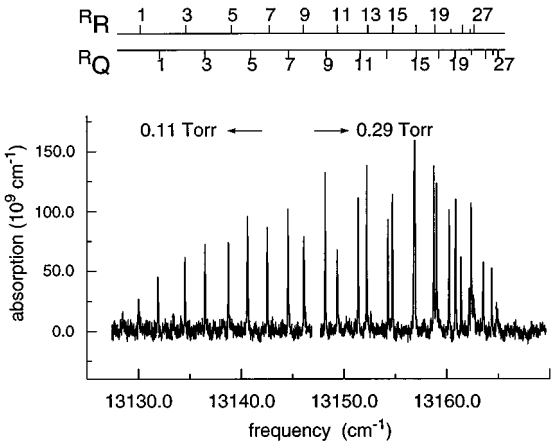

FIG. 2. CRD recording of both R branches of $^{18}O_2$. The two parts displayed here were recorded at different pressures, as indicated.

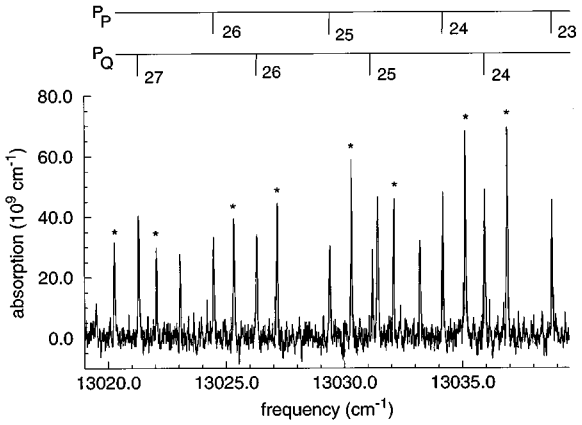

FIG. 3. Recording of the A band of $^{17}O_2$, at a pressure of 2.25 Torr of the ^{17}O-enriched sample. Lines of $^{16}O^{17}O$ are indicated by *. The remaining absorptions are due to $^{16}O_2$.

(CRDS) configuration. For the principles of CRDS we refer to the literature [9–14]. With highly reflecting mirrors of $R > 99.998\%$ (Research Electro Optics) a stable cavity (radius of curvature, 45 cm; mirror separation, 42 cm) is formed. Ring-down decay times of typically 100 μs (empty cavity) could be obtained. Decay transients were detected with a photomultiplier tube (Thorn EMI 9658RA) and stored on a 350-MHz oscilloscope (LeCroy 9450). After averaging signals from 10–30 laser pulses the decay transients were evaluated on-line by computer (Sun workstation). The resulting decay transient, measured as a function of wavelength setting, is an accurate and sensitive measure of the absorption in the cavity. The extremely long ring-down decay times obtained in our setup correspond to effective absorption path lengths of over 100 km (3τ). To keep the absorption in the linear regime, the oxygen gas pressure was regulated for recordings of weak and strong lines. As an example, a spectrum of the ^RR and ^RQ branches of $^{18}O_2$ is shown in Fig. 2,

TABLE I. Transition frequencies of $^{16}O^{18}O$ in cm^{-1}. Levels denoted by an asterisk do not exist due to constraints of angular-momentum coupling. Δ_{o-c} refers to the difference between the observed value and the calculated value determined by a least-squares fit of the molecular constants.

	^PQ		^PP		^RR		^RQ	
N	observed	Δ_{o-c}	observed	Δ_{o-c}	observed	Δ_{o-c}	observed	Δ_{o-c}
0	*	*	*	*	*	*	13 127.467	0.042
1	*	*	13 120.278	0.006	13 128.192	0.036		
2	13 119.616	−0.005	13 117.419	−0.050	13 130.608	0.000	13 132.549	0.010
3	13 116.589	−0.058	13 114.522	−0.056	13 132.994	0.023	13 134.932	0.004
4					13 135.249	0.003	13 137.238	0.016
5	13 110.530	−0.008	13 108.570	0.037	13 137.446	0.013	13 139.423	−0.001
6					13 139.525	−0.007		
7	13 104.104	−0.005	13 102.141	0.002			13 143.532	−0.026
8	13 100.756	−0.012	13 098.836	0.025	13 143.447	−0.015	13 145.482	−0.008
9	13 097.380	0.040	13 095.444	0.049	13 145.295	0.001	13 147.331	−0.002
10	13 093.853	0.026	13 091.865	−0.028	13 147.043	0.006	13 149.069	−0.017
11	13 090.178	−0.049	13.088.249	−0.055	13 148.716	0.026	13 150.803	0.054
12	13 086.510	−0.031	13 084.598	−0.030	13 150.281	0.027		
13	13 082.792	0.024	13 080.833	−0.032	13 151.786	0.057	13 153.835	0.028
14	13 078.897	−0.012	13 077.003	−0.012	13 153.147	0.033	13 155.202	0.001
15	13 074.949	−0.014	13 073.080	0.001	13 154.409	0.000	13 156.499	−0.006
16	13 070.947	0.016	13 069.064	0.008	13 155.614	0.000		
17	13 066.844	0.032						
18			13 060.759	0.009				
19	13 058.275	−0.040	13 056.425	−0.042				
20	13 053.885	−0.053	13 052.052	−0.046	13 159.519	−0.014		
21	13 049.491	0.018	13 047.666	0.024				
22	13 044.945	0.022	13 043.127	0.027				

TABLE II. Transition frequencies of $^{16}O^{17}O$ in cm^{-1}. Levels denoted by an asterisk do not exist due to constraints of angular-momentum coupling. Δ_{o-c} refers to the difference between the observed value and the calculated value determined by a least-squares fit of the molecular constants.

	^PQ		^PP		^RR		^RQ	
N	observed	Δ_{o-c}	observed	Δ_{o-c}	observed	Δ_{o-c}	observed	Δ_{o-c}
0	*	*	*	*	*	*	13 126.493	−0.015
1	*	*	13 119.231	0.010	13 127.328	0.005	13 129.221	0.014
2	13 118.510	0.004	13 116.336	−0.005	13 129.871	0.029	13 131.798	0.029
3	13 115.444	−0.003	13 113.361	−0.009	13 132.290	0.019	13 134.213	−0.012
4	13 112.298	−0.046	13 110.298	−0.011	13 134.591	−0.019	13 136.574	−0.009
5	13 109.180	0.013	13 107.177	0.018	13 136.849	−0.008	13 138.867	0.020
6	13 105.906	−0.001	13 103.928	0.009	13 139.035	0.021	13 141.051	0.034
7	13 102.549	−0.012	13 100.571	−0.018	13 141.051	−0.028	13 143.120	0.025
8	13 099.113	−0.015	13 097.160	−0.010	13 143.120	0.068	13 145.108	0.027
9	13 095.605	−0.001	13 093.672	0.011	13 144.968	0.033	13 146.996	0.022
10	13 092.010	0.014	13 090.069	0.007	13 146.746	0.021	13 148.766	−0.009
11	13 088.291	−0.006	13 086.345	−0.029	13 148.424	0.001	13 150.464	−0.019
12	13 084.501	−0.007	13 082.582	−0.015	13 149.999	−0.029	13 152.061	−0.037
13	13 080.641	0.010	13 078.737	0.008	13 151.510	−0.031	13 153.595	−0.026
14	13 076.649	−0.015	13 074.770	−0.002	13 152.941	−0.021	13 155.067	0.016
15	13 072.609	0.001	13 070.704	−0.022	13 154.286	−0.003	13 156.408	0.021
16	13 068.451	−0.012	13 066.603	0.013	13 155.541	0.019		
17	13 064.215	−0.013	13 062.356	−0.008				
18	13 059.892	−0.011	13 058.021	−0.028				
19	13 055.486	−0.003	13 053.638	−0.005				
20	13 050.995	0.010	13 049.166	0.018				
21	13 046.400	0.010	13 044.588	0.025				
22	13 041.716	0.010	13 039.889	0.002				
23	13 036.933	0.001	13 035.126	0.004				
24	13 032.057	−0.010	13 030.261	−0.005				
25	13 027.142	0.030	13 025.328	0.009				
26	13 022.075	0.009	13 020.289	0.007				
27	13 016.919	−0.011	13 015.149	−0.005				
28	13 011.700	−0.002	13 009.921	−0.014				
29	13 006.392	0.008	13 004.624	−0.001				
30	13 000.977	0.003	12 999.243	0.020				
31	12 995.473	0.001	12 993.726	−0.004				
32	12 989.888	0.009	12 988.156	0.011				
33	12 984.172	−0.022	12 982.427	−0.042				

with adjacent parts recorded at different pressures. Spectra of O_2 isotopomers were recorded, either from natural O_2-gas samples, a ^{18}O-enriched sample (Euriso Top, 95% $^{18}O_2$) also containing $^{17}O^{18}O$ and $^{16}O^{18}O$, or a ^{17}O-enriched sample (Campro Scientific 50% ^{17}O-atom) also containing $^{16}O^{17}O$. A spectrum of the A band for $^{17}O_2$ is shown in Fig. 3. Lines pertaining to $^{16}O^{17}O$ and $^{16}O_2$ are also present.

Since absolute frequency calibration of pulsed near-infrared lasers is not straightforward, we choose to pump a dye laser in the range 577–587 nm and then employ Raman shifting in H_2 to cover the wavelength range 759–775 nm. The visible output of the dye laser can easily be calibrated against the I_2-reference standard [15]. For this purpose the I_2-absorption spectrum (in linear absorption) and the dye laser power are measured simultaneously with the CRD spectrum of O_2 isotopomers. Before further analysis the I_2 spectrum is normalized to the power spectrum of the dye laser. Absolute frequency positions of O_2 lines are obtained from computerized fitting of both spectra and subsequent interpolation. The Raman shift Ω, which slightly depends on the H_2-gas density in the Raman cell, is evaluated with $\Omega(p) = \Omega_0 + \alpha p + \beta p^2$, where $\Omega_0 = 4155.2547\ cm^{-1}$, $\alpha = -3.38 \times 10^{-3}\ cm^{-1}\,amagat^{-1}$, $\beta = 4.1 \times 10^{-6}\ cm^{-1}\,amagat^{-2}$, and p is the H_2 density in amagat [16]. Various densities of 10–25 amagat were used in the Raman shifter.

The linewidth of the laser source is $0.06\ cm^{-1}$ and the bandwidth of the Raman-shifted frequency was found to be the same. Under the chosen pressure conditions in the CRD cell of 0.1–20 Torr, collisional broadening can be neglected. The I_2 calibrations were performed in low-pressure samples,

TABLE III. Transition frequencies of $^{18}O_2$ in cm^{-1}. Levels denoted by an asterisk do not exist due to constraints of angular-momentum coupling. Δ_{o-c} refers to the difference between the observed value and the calculated value determined by a least-squares fit of the molecular constants.

	^PQ		^PP		^RR		^RQ	
N	observed	Δ_{o-c}	observed	Δ_{o-c}	observed	Δ_{o-c}	observed	Δ_{o-c}
1	*	*	13 122.536	−0.001	13 129.957	−0.001	13 131.869	0.002
3	13 119.341	0.110	13 117.228	0.050	13 134.491	−0.001	13 136.458	0.001
5	13 113.514	0.026	13 111.473	−0.018	13 138.697	0.001	13 140.692	0.002
7	13 107.497	0.054	13 105.536	0.060	13 142.565	−0.002	13 144.588	0.003
9	13 101.116	0.039	13 099.160	0.027	13 146.100	−0.004	13 148.139	−0.002
11	13 094.455	0.069	13 092.524	0.061	13 149.303	−0.002	13 151.362	0.001
13	13 087.401	0.031	13 085.498	0.033	13 152.170	0.001	13 154.244	0.001
15	13 080.057	0.030	13 078.165	0.026	13 154.725	0.030	13 156.821	0.034
17	13 072.386	0.030	13 070.511	0.026	13 156.909	0.029	13 159.010	0.022
19	13 064.397	0.040	13 062.549	0.047	13 158.746	0.024	13 160.860	0.014
21	13 055.977	−0.052	13 054.178	−0.012	13 160.245	0.026	13 162.377	0.018
23	13 047.406	0.035	13 045.580	0.032	13 161.394	0.026	13 163.548	0.024
25	13 038.441	0.059	13 036.628	0.053	13 162.185	0.018	13 164.374	0.035
27	13 029.114	0.053	13 027.230	−0.039	13 162.622	0.010	13 164.822	0.022
29	13 019.417	0.011	13 017.655	0.025			13 164.917	0.012
31	13 009.462	0.045	13 007.692	0.036				
33	12 999.085	−0.005	12 997.369	0.025				
35	12 988.422	−0.003	12 986.698	0.003				
37	12 977.423	0.003	12 975.706	0.001				
39	12 966.097	0.025	12 964.361	−0.011				
41	12 954.359	−0.020	12 952.659	−0.035				
43	12 942.170	−0.169	12 940.603	−0.066				

where typical linewidths of $0.07\ cm^{-1}$ were obtained. The estimated uncertainty in our frequency determination is $0.02–0.03\ cm^{-1}$ and up to $0.05\ cm^{-1}$ for overlapping and very weak lines.

III. SPECTROSCOPIC RESULTS ON $^{16}O^{18}O$, $^{16}O^{17}O$, $^{18}O_2$, $^{17}O^{18}O$, AND $^{17}O_2$

From series of CRD recordings, using low- and high-pressure samples of natural O_2 and ^{18}O- and ^{17}O-enriched samples, we derived data on the transition frequencies of the $b\,^1\Sigma_g^+ - X\,^3\Sigma_g^-$ (0,0) band. The results for $^{16}O^{18}O$, $^{16}O^{17}O$, $^{18}O_2$, $^{17}O^{18}O$, and $^{17}O_2$ are collected in Tables I–V, respectively. Since the resolution in our experiment does not make an improvement over existing data for $^{16}O_2$ [8,17], we do not include these. During the final analysis of our measurements, highly accurate data on the A band of $^{18}O_2$ were reported [18]. Since these data were limited to 15 transitions we decided to report here on our extended analysis of 72 lines for $^{18}O_2$. Transitions in the four magnetic dipole-allowed branches (see Fig. 4 for an energy-level scheme) were determined. For $^{18}O_2$, similar to $^{16}O_2$, transitions originating in the even rotational states are forbidden. This is not the case for $^{17}O_2$, where a 7:5 ratio is found between odd and even N, due to the nuclear spin of 5/2 for the ^{17}O nucleus, nor the case for the heteronuclear isotopomers.

For each isotopomer the data were incorporated in a least-squares minimization routine to derive molecular constants. For the $X\,^3\Sigma_g^-(v=0,N,J)$ state, the effective Hamiltonian of Rouillé *et al.* [19] was adopted, while for the $b\,^1\Sigma_g^+(v=0,N)$ excited states, we used

$$E(N)=\nu_0+B'N(N+1)-D'N^2(N+1)^2, \qquad (1)$$

where ν_0 is the band origin, B' the rotational constant, and D' the centrifugal distortion parameter. Accurate spectroscopic studies on the $X\,^3\Sigma_g^-$, $v=0$ state have been per-

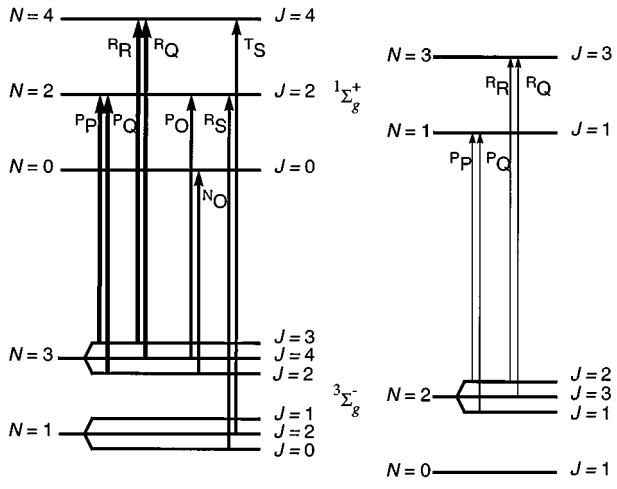

FIG. 4. Energy-level scheme of molecular oxygen with the $X\,^3\Sigma_g^-$ ground and $b\,^1\Sigma_g^+$ excited state. On the left side the symmetry-allowed levels in $^{16}O_2$ and $^{18}O_2$ are shown with the four magnetic dipole branches (^PP, ^PQ, ^RR, and ^RQ) as well as the four electric quadrupole branches (^PO, ^NO, ^RS, and ^TS). On the right side the symmetry-forbidden levels and transitions are shown; note that these are allowed for isotopomers other than $^{16}O_2$ and $^{18}O_2$.

TABLE IV. Transition frequencies of $^{17}O^{18}O$ in cm^{-1}. Levels denoted by an asterisk do not exist due to constraints of angular-momentum coupling. Δ_{o-c} refers tof the difference between the observed value and the calculated value determined by a least-squares fit of the molecular constants.

	^PQ		^PP		^RR		^RQ	
N	observed	Δ_{o-c}	observed	Δ_{o-c}	observed	Δ_{o-c}	observed	Δ_{o-c}
0	*	*	*	*	*	*	13 128.512	0.042
1	*	*	13 121.536	0.068	13 129.136	0.029	13 131.029	0.021
2	13 120.932	0.043	13 118.723	−0.030	13 131.507	0.023	13 133.445	0.024
3	13 117.986	−0.027	13 115.901	−0.052	13 133.785	0.009	13 135.737	0.001
4	13 115.033	−0.059	13 113.002	−0.066	13 135.978	−0.004	13 137.967	0.007
5	13 112.035	−0.065	13 110.112	0.012	13 138.102	−0.001		
6	13 109.046	0.016	13 107.099	0.052				
7	13 105.921	0.043	13 103.953	0.043			13 144.088	−0.018
8	13 102.667	0.023			13 143.930	−0.023	13 145.971	−0.010
9	13 099.333	0.006			13 145.711	−0.019	13 147.764	−0.004
10	13 095.943	0.017	13 094.008	0.016	13 147.402	−0.019		
11			13 090.460	−0.058			13 151.124	0.041
12	13 088.811	−0.061	13 086.904	−0.055	13 150.577	0.035	13 152.644	0.035
13	13 085.207	−0.012	13 083.307	−0.008	13 152.003	0.031	13 154.062	0.015
14	13 081.445	−0.037	13 079.575	−0.012	13 153.316	0.003		
15	13 077.636	−0.024	13 075.761	−0.013	13 154.591	0.024		
16	13 073.740	−0.013	13 071.876	0.000	13 155.733	0.001		
17	13 069.763	0.002	13 067.892	0.000				
18	13 065.686	0.002	13 063.891	0.067				
19	13 061.523	0.002	13 059.635	−0.035				
20	13 057.241	−0.032	13 055.370	−0.060				
21	13 052.901	−0.038	13 051.108	0.004				
22	13 048.562	0.043	13 046.741	0.049				
23	13 044.087	0.075	13 042.258	0.065				
24	13 039.456	0.037	13 037.628	0.020				
25	13 034.671	−0.067	13 032.868	−0.068				
26	13 029.914	−0.057	13 028.153	−0.023				
27	13 025.164	0.049						

formed for all isotopomers except $^{17}O_2$. The results from microwave, far-infrared, laser magnetic resonance (LMR), and Raman spectroscopic studies yielded a better accuracy for the ground-state molecular constants than the present electronic excitation. Therefore these constants were kept fixed in the fitting routines at accurate values from the literature. These ground-state constants are listed in Table VI. The data on the $b\,^1\Sigma_g^+ - X\,^3\Sigma_g^-$ (0,0) band of $^{16}O_2$ from Babcock and Herzberg [17] and Brault [8] were reanalyzed with updated constants for the ground state. These were obtained from the study of Rouillé *et al.* [19], in which data from the LMR study of Mizushima *et al.* [20] and the far-infrared study of Zink and Mizushima [21] were included. For $^{16}O^{18}O$ and $^{18}O_2$ the constants of Steinbach and Gordy [22] were used, while for $^{16}O^{17}O$ and $^{17}O^{18}O$ the constants of Cazolli *et al.* [23] were adopted. In the fit for $^{18}O_2$ the data of Gagliardi *et al.* [18], with an accuracy of 10^{-3} cm^{-1}, were included. For the $^{17}O_2$ isotopomer no data were available, and therefore also the ground-state constants were varied in the minimization routine. The spin coupling constants λ_0 and μ_0 for $^{17}O_2$ were estimated from the values for the other isotopomers. These values are listed in Table VI as well.

Resulting molecular constants for the $b\,^1\Sigma_g^+$, $v=0$ excited state are presented in Table VII for all isotopomers. In all cases an unperturbed molecular band structure was found. The deviations from the least-squares fit for each line are included in the Tables I–V. Consistency is found with the average estimated uncertainty of 0.03 cm^{-1} for the transition frequencies, resulting in a χ^2 per data point of 1.0. The band origin ν_0 is for all isotopomers chosen as the difference between the $N=0$ level in the $b\,^1\Sigma_g^+$, $v=0$ state and the $N=0$, $J=0$ level in the electronic ground state. Although the latter level is nonexisting, this definition provides the best basis for a comparison in terms of a pure isotope shift.

IV. RELEVANCE FOR TESTS OF THE SYMMETRIZATION POSTULATE IN $^{16}O_2$

In their search for a possible violation of the symmetrization postulate, de Angelis *et al.* [2] probed the expected position for the $^RR(4)$ line of the $b-X(0,0)$ band, while Hilborn and Yuca [3] searched for the $^PQ(22)$ [24] line. Upper limits were determined at 5×10^{-7} [2] and 8×10^{-7} [3], respectively. Study of the less abundant isotopomers of oxygen is of importance for tests of the symmetrization postulate in $^{16}O_2$. First of all, the weak line intensities of the rare isotopomers can provide a sensitivity scale. The dynamic range of many detectors is limited to a few orders of magnitude and Beer's law for direct absorption is only linear in the limit of

TABLE V. Transition frequencies of $^{17}O_2$ in cm^{-1}. Levels denoted by an asterisk do not exist due to constraints of angular-momentum coupling. Δ_{o-c} refers to the difference between the observed value and the calculated value determined by a least-squares fit of the molecular constants.

	^PQ		^PP		^RR		^RQ	
N	observed	Δ_{o-c}	observed	Δ_{o-c}	observed	Δ_{o-c}	observed	Δ_{o-c}
0	*	*	*	*	*	*	13 127.558	0.010
1	*	*	13 120.421	0.008	13 128.300	0.032	13 130.191	0.030
2	13 119.760	−0.010	13 117.591	−0.028	13 130.729	0.018	13 132.656	0.013
3	13 116.796	−0.011	13 114.745	0.006	13 133.084	0.018	13 134.998	−0.025
4	13 113.794	−0.007	13 111.734	−0.037	13 135.324	−0.010	13 137.325	0.015
5	13 110.714	−0.007	13 108.736	0.019	13 137.520	0.007	13 139.512	0.008
6	13 107.569	0.008	13 105.596	0.021	13 139.610	0.006	13 141.612	0.003
7	13 104.317	0.000	13 102.337	−0.009	13 141.612	0.006	13 143.654	0.031
8	13 100.973	−0.015	13 099.016	−0.015	13 143.553	0.033	13 145.577	0.029
9	13 097.555	−0.018	13 095.605	−0.023	13 145.373	0.028	13 147.401	0.017
10	13 094.071	−0.002	13 092.158	0.019	13 147.110	0.029	13 149.126	−0.004
11	13 090.502	0.016	13 088.560	−0.003	13 148.766	0.038	13 150.755	−0.032
12	13 086.796	−0.017	13 084.885	−0.015	13 150.244	−0.041	13 152.327	−0.026
13	13 083.053	0.000	13 081.165	0.015	13 151.732	−0.020	13 153.797	−0.033
14	13 079.215	0.008	13 077.304	−0.009	13 153.108	−0.022	13 155.232	0.016
15	13 075.269	−0.005	13 073.385	−0.005	13 154.420	0.003		
16	13 071.239	−0.016	13 069.358	−0.022	13 155.630	0.017		
17	13 067.145	−0.004	13 065.282	0.000				
18	13 062.950	−0.006	13 061.101	0.003				
19	13 058.668	−0.008	13 056.819	−0.008				
20	13 054.295	−0.013	13 052.494	0.026				
21	13 049.871	0.017	13 048.020	−0.002				
22	13 045.345	0.032	13 043.522	0.033				
23	13 040.693	0.009	13 038.868	−0.001				
24	13 035.959	−0.008	13 034.165	0.004				
25	13 031.156	−0.007	13 029.349	−0.016				
26	13 026.280	0.008	13 024.477	−0.005				
27	13 021.323	0.031	13 019.509	−0.001				
28	13 016.229	0.005	13 014.452	0.001				
29	13 011.059	−0.010	13 009.298	−0.005				
30	13 005.835	0.011	13 004.052	−0.015				
31	13 000.482	−0.009	12 998.773	0.031				
32	12 995.053	−0.017	12 993.328	−0.001				

TABLE VI. Molecular constants for the $X\,^3\Sigma_g^-$, $v=0$ ground state of molecular oxygen, which were kept fixed in our analysis, obtained from the literature. For $^{17}O_2$ the rotational and centrifugal distortion constant were derived in the present study. Vaues for the spin-coupling parameters were estimated. All values are in cm^{-1}. The value in parentheses represents the uncertainly (international standard deviation) in units of the last significant digit.

	$^{16}O_2$	$^{16}O^{17}O$	$^{16}O^{18}O$	$^{17}O^{18}O$	$^{18}O_2$	$^{17}O_2$
B_0	1.437 676 476(77)	1.395 319(3)	1.357 853 0(3)	1.315 490(3)	1.278 008 47(23)	1.352 89(2)
D_0	$4.842\,56(63)\times10^{-6}$	4.623×10^{-6}	4.302×10^{-6}	4.102×10^{-6}	3.835×10^{-6}	$4.29(5)\times10^{-6}$
H_0	$2.8(16)\times10^{-12}$					
λ_0	1.984 751 322(72)	1.984 709 4(3)	1.984 676 2(14)	1.984 632 9(13)	1.984 596 22(37)	1.984 676 2[a]
λ_0'	$1.945\,21(50)\times10^{-6}$	$1.917(6)\times10^{-6}$	$1.771(26)\times10^{-6}$	$1.801(10)\times10^{-6}$	$1.738(14)\times10^{-6}$	1.8[a]
λ_0''	$1.103(41)\times10^{-11}$					
μ_0	$-8.425\,390(13)\times10^{-3}$	$-8.176\,12(13)\times10^{-3}$	$-7.955\,1(23)\times10^{-3}$	$-7.706\,96(23)\times10^{-3}$	$-7.486\,48(10)\times10^{-3}$	-7.9×10^{-3} [a]
μ_0'	$-8.106(32)\times10^{-9}$	$-8.0(10)\times10^{-9}$	$-2.06(38)\times10^{-9}$	$-9.0(20)\times10^{-9}$	$-11.7(18)\times10^{-9}$	-8.0×10^{-9} [a]
μ_0''	$-4.7(19)\times10^{-14}$					
Ref.	[19]	[23]	[22]	[23]	[22]	This work

[a]Constants fixed in the fit at these estimated values.

TABLE VII. Molecular constants for the $b\,^1\Sigma_g^+$, $v=0$ excited state of molecular oxygen. The constants for the $^{16}O_2$ and $^{16}O^{17}O$ isotopomer were derived from a reanalysis of the data of Refs. [8, 17]. All values are in cm^{-1}. The value in parentheses represents the estimated error (international standard deviation) from the fit in units of the last digit.

	$^{16}O_2$	$^{16}O^{17}O$	$^{16}O^{18}O$	$^{17}O^{18}O$	$^{18}O_2$	$^{17}O_2$
ν_0	13 122.6903(7)	13 123.808(3)	13 124.797(7)	13 125.924(8)	13 126.932 7(8)	13 124.931(8)
B'	1.391 251 83(10)	1.350 232(15)	1.313 92(9)	1.273 19(8)	1.236 833(6)	1.309 16(3)
D'	$5.360(1)\times10^{-6}$	$5.07(2)\times10^{-6}$	$4.4(2)\times10^{-6}$	$4.8(1)\times10^{-6}$	$4.255(8)\times10^{-6}$	$4.68(8)\times10^{-6}$

weak absorption. Searches for violation of the symmetrization postulate at the intensity level of 10^{-8} and beyond require an intensity scale over many orders of magnitude. Weak resonances pertaining to rare isotopomers in a gas sample can be used for this purpose. Because the line strengths of the various isotopomers can in first order be considered equal, the abundances themselves reflect the intensity levels to be obtained in measurements of natural gas. The natural abundances of atomic ^{18}O and ^{17}O are 0.20% and 0.037%, respectively. From these values the natural abundances of all isotopomer molecules can be calculated. Resulting values are listed in Table VIII. It is taken into account that the symmetry-allowed states in $^{16}O_2$ and $^{18}O_2$ have double occupancy, because half of the states are symmetry forbidden. In $^{17}O_2$ there is a 7:5 ratio between odd and even rotational states. The sensitivity scale can be extended to lower values if electric quadrupole transitions are considered. Brault succeeded in recording several quadrupole transitions in $^{16}O_2$ from long path-length spectroscopic studies of the Earth's atmosphere and determined their relative intensity, with respect to magnetic dipole transitions, at 3×10^{-6} [8]. The combination of natural isotopic abundances and quadrupole or dipole line strengths provides a sensitivity scale of 13 orders of magnitude, as given in Table VIII. Fine tuning between the gaps on this scale is possible via calculable relative populations of rotational states in a room-temperature gas sample. From such calculations it follows that the $^PQ(22)$ line, sought by Hilborn and Yuca [3,24], is a factor of 5 weaker than the $^PQ(8)$ line in the same branch.

In this work we have recorded spectra of the $b-X(0,0)$ band for the $^{17}O^{18}O$ and $^{17}O_2$ isotopomers, while improved analysis has been presented for the other isotopomers. Knowledge of the spectral positions of the isotopomer lines prevents erroneous interpretation of weak signals. From our analysis it follows that the $^RR(3)$ line of $^{17}O^{18}O$ lies at 13 133.78 cm^{-1}, while the $^RR(4)$ line of $^{16}O_2$ is expected at 13 133.89 cm^{-1}. The separation is only 3 GHz, while the linewidth in the absorption spectrum of de Angelis *et al.* [2] equals this value when the side lobes occurring in frequency-modulated spectra are included. We note that the relative abundance of $^{17}O^{18}O$ in natural O_2 is 7.5×10^{-7}, just at the detection limit claimed by de Angelis *et al.* Near the symmetry-forbidden magnetic dipole $^RR(4)$ line of $^{16}O_2$ is a $^RS(3)$ electric quadrupole line. These electric quadrupole transitions, calculated from the molecular constants of Tables VI and VII, are presented in Table IX. The $^RS(3)$ line, separated by 10 GHz from the $^RR(4)$ line, should be observable at the 3×10^{-6} level, which is a factor of 6 above the detection limit in the experiment of de Angelis *et al.*

The $^PQ(22)$ line, sought by Hilborn and Yuca [3,24] is not overlapped by any of the isotopomer lines. The $^PQ(20)$ line, initially referred to as the searched for line in Ref. [3], coincides with the $^PP(21)$ line of $^{16}O^{18}O$. At a sensitivity level of 8×10^{-7} this $^{16}O^{18}O$ isotopomer line should appear with a signal-to-noise ratio of 5000 at the search position of the symmetry-forbidden $^{16}O_2$ $^PQ(20)$ line.

For the convenience of future use, the symmetry-forbidden lines of $^{16}O_2$ are listed in Table X. The fact that these frequencies are accurately known makes the $^{16}O_2$ di-

TABLE VIII. Relative intensity scale of transitions in O_2 isotopomers.

Isotopomer	Transition	Relative strength
$^{16}O_2$	magnetic dipole	1
$^{16}O^{18}O$	magnetic dipole	2×10^{-3}
$^{16}O^{17}O$	magnetic dipole	4×10^{-4}
$^{18}O_2$	magnetic dipole	4×10^{-6}
$^{16}O_2$	electric quadrupole	3×10^{-6}
$^{17}O^{18}O$	magnetic dipole	7×10^{-7}
$^{17}O_2$	magnetic dipole	1×10^{-7}
$^{16}O^{18}O$	electric quadrupole	6×10^{-9}
$^{16}O^{17}O$	electric quadrupole	1×10^{-9}
$^{18}O_2$	electric quadrupole	1×10^{-11}
$^{17}O^{18}O$	electric quadrupole	2×10^{-12}
$^{17}O_2$	electric quadrupole	3×10^{-13}

TABLE IX. Calculated transition frequencies in cm^{-1} for electric quadrupole transitions in $^{16}O_2$.

N	^PO	^NO	^RS	^TS
1	13 119.91		13 129.26	13 147.73
3	13 113.95	13 105.74	13 133.56	13 164.03
5	13 107.59	13 088.14	13 138.22	13 179.91
7	13 100.85	13 070.21	13 142.53	13 195.40
9	13 093.74	13 051.93	13 146.48	13 210.50
11	13 086.25	13 033.28	13 150.05	13 225.21
13	13 078.40	13 014.28	13 153.24	13 239.52
15	13 070.17	12 994.93	13 156.05	13 253.43
17	13 061.58	12 975.22	13 158.47	13 266.93
19	13 052.61	12 955.16	13 160.51	13 280.03
21	13 043.27	12 934.74	13 162.16	13 292.71
23	13 033.56	12 913.97	13 163.41	13 304.98
25	13 023.48	12 892.85	13 164.27	13 316.82
27	13 013.02	12 871.38	13 164.72	13 328.23
29	13 002.18	12 849.56	13 164.77	13 339.21

TABLE X. Tabulated transition frequencies in cm^{-1} for symmetry-forbidden magnetic dipole transitions in $^{16}O_2$.

N	^PQ	^PP	^RR	^RQ
0				13 125.47
2	13 117.24	13 115.07	13 128.98	13 130.90
4	13 110.89	13 108.85	13 133.89[a]	13 135.86
6	13 104.26	13 102.27	13 138.43	13 140.43
8	13 097.27	13 095.31	13 142.59	13 144.62
10	13 089.93	13 087.99	13 146.37	13 148.43
12	13 082.21	13 080.30	13 149.78	13 151.85
14	13 074.13	13 072.24	13 152.80	13 154.89
16	13 065.68	13 063.81	13 155.44	13 157.55
18	13 056.86	13 055.01	13 157.69	13 159.82
20	13 047.67	13 045.84	13 159.55	13 161.70
22	13 038.11[b]	13 036.30	13 161.02	13 163.19
24	13 028.18	13 026.38	13 162.09	13 164.28
26	13 017.87	13 016.09	13 162.77	13 164.97
28	13 007.19	13 005.43	13 063.04	13 165.26
30	12 996.13	12 994.39	13 062.90	13 165.14

[a]Line sought by de Angelis *et al.* [2].
[b]Line sought by Hilborn and Yuca [3,24].

atomic homonuclear molecule a suitable candidate to study fundamental physics. Symmetry-forbidden lines can be searched for at a well-established frequency position.

V. EXPERIMENTAL SENSITIVITY

The noise equivalent detection limit in our present CRD setup was determined from a measurement of a quadrupole line in the ^TS branch. The electric quadrupole lines are well suited to a sensitivity determination, since they lie at the blue side of all magnetic dipole lines. Also no interference with the (1,1) band occurs at these frequencies. For the spectroscopic measurements aimed at a high sensitivity we used an average of 12 decay times (after signal summation over ten laser shots for each decay) at each wavelength position in search of the $^TS(9)$ electric quadrupole transition at 600 Torr pressure. The result of this procedure is shown in Fig. 5. By interpolation with a simultaneously recorded I_2 spectrum, a weak resonance is observed at a frequency of 13 210.51 cm^{-1}, determined by a computerized fit of a Voigt profile with an oscillatory background. The background level is mainly due to the reflectivity of the mirrors in our setup, while at 600-Torr gas pressures, extinction due to Rayleigh scattering is also observed. The oscillation at an absorption level of 3×10^{-9} cm^{-1} corresponds to an effective variation of 10^{-7} in the mirror reflectivity. Oscillations of the background are also observed in other CRD studies; their origin, however, is not understood. It is verified that the weak resonance is reproducible and disappears in an empty cavity, while the oscillatory background remains. The molecular constants for $^{16}O_2$ predict a line at 13 210.50 cm^{-1} (see Table IX, where we have listed calculated positions of quadrupole lines). In view of the 0.05-cm^{-1} error margin for this weak and pressure-broadened line, the observed resonance perfectly coincides with $^TS(9)$. Also the width (full width at half maximum of 0.1 cm^{-1}) and intensity (2×10^{-9} cm^{-1})

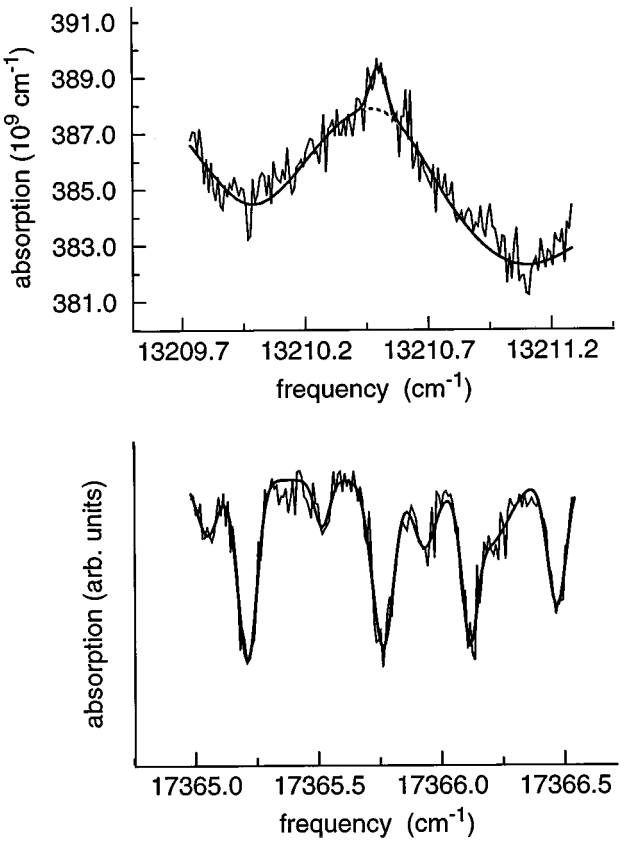

FIG. 5. Upper trace: observed spectrum of the $^TS(9)$ electric quadrupole line of $^{16}O_2$ superimposed on an oscillatory background, due to a variation of the background loss in the CRD setup. Lower trace: a simultaneously recorded I_2 absorption spectrum with the fundamental output of the dye laser. The O_2 spectrum is Raman-shifted by 4155.24 cm^{-1} with respect to the calibration spectrum.

are in good agreement with the expected values. From the observation of this quadrupole line, at a signal-to-noise ratio (SNR) of 2, we estimate that our sensitivity in performing a test on the symmetrization postulate is 1.5×10^{-6} with respect to a magnetodipole transition of $^{16}O_2$. Compared to the previous tests the sensitivity for a test of the symmetrization postulate is only slightly lower than in Refs. [2] and [3].

We attempted to observe some ^RR lines at $N=9-13$ of $^{18}O_2$ in natural O_2 gas. Although the lines should have intensities at the 4×10^{-6} level, they were obscured by the strong Lorentzian wings of the nearby $^{16}O_2$ lines, and were therefore not observed.

We note that, in fact, the work of Brault [8] represents the highest sensitivity study of molecular oxygen. Quadrupole lines were recorded from 43-atm km oxygen samples in the sunset spectrum of the Earth's atmosphere, with a SNR of 100. This corresponds to a 3×10^{-8} sensitivity, which is more than an order of magnitude better than all laboratory studies of molecular oxygen using lasers, including the present study and the studies of Refs. [2] and [3]. However, the method of Fourier-transform spectroscopy in the Earth's atmosphere was not used to search for symmetry-forbidden lines.

VI. CONCLUSION

In the present work, frequency positions and molecular constants for the oxygen *A* band have been determined for all isotopomers. We were able to record a positive signal on a line at the 3×10^{-6} sensitivity level, thus demonstrating the sensitivity of our cavity-ring-down setup. The use of a sensitivity scale of 13 orders of magnitude is presented, which is practical for future test experiments. This scale, based on isotopic abundances, electric quadrupole line strengths, and Boltzman populations, gives the possibility of recording a positive signal (resonance line) at each desired intensity level. The spectroscopic information on isotopomers and also the electric quadrupole lines presented here, provides insight into the occurrence of coincidences at search positions for symmetry-forbidden lines with weak allowed resonances.

ACKNOWLEDGMENTS

The authors acknowledge financial support from the Space Research Organization Netherlands (SRON) and from the Netherlands Foundation for Fundamental Research of Matter (FOM). They wish to thank G. Meijer (KUN, Nijmegen) for stimulating discussions.

[1] K. J. Ritter and T. D. Wilkinson, J. Mol. Spectrosc. **121**, 1 (1987).
[2] M. de Angelis, G. Gagliardi, L. Gianfrani, and G. M. Tino, Phys. Rev. Lett. **76**, 2840 (1996).
[3] R. C. Hilborn and C. L. Yuca, Phys. Rev. Lett. **76**, 2844 (1996).
[4] G. H. Dieke and H. D. Babcock, Proc. Natl. Acad. Sci. USA **13**, 670 (1927).
[5] W. Heisenberg, Z. Phys. **41**, 239 (1927).
[6] G. Herzberg, *Spectra of Diatomic Molecules* (Grieger, Malabar, Fla, 1991).
[7] P. R. Bunker, *Molecular Symmetry and Spectroscopy* (Academic Press, New York, 1979).
[8] J. W. Brault, J. Mol. Spectrosc. **80**, 384 (1980).
[9] A. O'Keefe and D. A. G. Deacon, Rev. Sci. Instrum. **59**, 2544 (1988).
[10] G. Meijer, M. G. H. Boogaarts, R. T. Jongma, D. H. Parker, and A. M. Wodtke, Chem. Phys. Lett. **217**, 112 (1994).
[11] D. Romanini and K. K. Lehmann, J. Chem. Phys. **99**, 6287 (1993).
[12] P. Zalicki and R. N. Zare, J. Chem. Phys. **102**, 2708 (1995).
[13] A. O. Keefe, J. J. Scherer, A. L. Cooksky, R. Sheeks, J. Heath, and R. J. Saykally, Chem. Phys. Lett. **172**, 214 (1990).
[14] B. A. Paldus, J. S. Harris, Jr., J. Martin, J. Xie, and R. N. Zare, J. Appl. Phys. **92**, 3199 (1997).
[15] S. Gerstenkorn and P. Luc, *Atlas du Spectre d'Absorption de la Molecule de l'Iode entre 14800–20000 cm^{-1}* (CNRS, Paris, 1978).
[16] L. A. Rahn and G. J. Rosasco, Phys. Rev. A **41**, 3698 (1990).
[17] H. B. Babcock and L. Herzberg, Astrophys. J. **108**, 167 (1948).
[18] G. Gagliardi, L. Gianfrani, and G. M. Tino, Phys. Rev. A **55**, 4597 (1997).
[19] G. Rouillé, G. Millot, R. Saint-Loup, and H. Berger, J. Mol. Spectrosc. **154**, 372 (1992).
[20] M. Mizushima, L. Zink, and K. Evenson, J. Mol. Spectrosc. **107**, 395 (1984).
[21] L. Zink and M. Mizushima, J. Mol. Spectrosc. **125**, 154 (1987).
[22] W. Steinbach and W. Gordy, Phys. Rev. A **11**, 729 (1975).
[23] G. Cazolli, C. Degli Esposti, P. G. Favero, and G. Severi, Nuovo Cimento B **62**, 243 (1981).
[24] The authors of Ref. [3] have informed us that it was not the $^PQ(20)$ symmetry forbidden line that was sought, as mentioned in their paper, but the $^PQ(22)$ line; R. C. Hilborn (private communication).